

EVIDENCE OF VORTICITY AND SHEAR AT LARGE ANGULAR SCALES IN THE WMAP DATA: A VIOLATION OF COSMOLOGICAL ISOTROPY?

T. R. JAFFE¹, A. J. BANDAY¹, H. K. ERIKSEN², K. M. GÓRSKI^{3,4}, F. K. HANSEN²

Draft version October 29, 2018

ABSTRACT

Motivated by the large-scale asymmetry observed in the cosmic microwave background sky, we consider a specific class of anisotropic cosmological models – Bianchi type VII_h – and compare them to the *WMAP* first-year data on large angular scales. Remarkably, we find evidence of a correlation which is ruled out as a chance alignment at the 3σ level. The best fit Bianchi model corresponds to $x = 0.55$, $\Omega_0 = 0.5$, a rotation axis in the direction $(l, b) = (222^\circ, -62^\circ)$, shear $(\frac{\sigma}{H})_0 = 2.4 \times 10^{-10}$ and a right-handed vorticity $(\frac{\omega}{H})_0 = 6.1 \times 10^{-10}$. Correcting for this component greatly reduces the significance of the large-scale power asymmetry, resolves several anomalies detected on large angular scales (ie. the low quadrupole amplitude and quadrupole/octopole planarity and alignment), and can account for a non-Gaussian “cold spot” on the sky. Despite the apparent inconsistency with the best-fit parameters required in inflationary models to account for the acoustic peaks, we consider the results sufficiently provocative to merit further consideration.

Subject headings: cosmic microwave background — cosmology: observations — methods: numerical

1. INTRODUCTION

Despite initial reactions to the first year *WMAP*⁵ data – “the most revolutionary result is that there are no revolutionary results” (Bahcall 2003) – continued assessment has revealed some interesting discrepancies with the inferred best-fit, cosmological constant dominated, inflationary model of the primordial fluctuation spectrum.

A debate about the apparently low quadrupole amplitude (originally observed by *COBE*-DMR) has arisen (Efstathiou 2004) along with claims about other anomalies on large angular scales. de Oliveira-Costa et al. (2004) demonstrated a curious planarity and alignment of the quadrupole and octopole. In addition, Vielva et al. (2004) and Cruz et al. (2005) have detected a localised source of non-Gaussianity, in the form of a very cold spot on the sky of angular scale $\sim 10^\circ$. Of particular interest to us, however, was the discovery of a remarkable asymmetry in large-scale power as measured in the two hemispheres of a particular reference frame. (Eriksen et al. 2004a; Hansen et al. 2004a,b). It remains unclear why this was not detected by the bipolar power spectrum of Hajian, Souradeep, & Cornish (2005). Nevertheless, this has provided the motivation to investigate anisotropic cosmological models.

Following Bunn, Ferreira, & Silk (1996) and Kogut et al. (1997), we focus on a specific class of models – Bianchi type VII_h (Barrow et al. 1985). Such models were previously compared to the *COBE*-DMR

data in Kogut et al. (1997), where limits on the shear $(\frac{\sigma}{H})_0 < 10^{-9}$ and vorticity $(\frac{\omega}{H})_0 < 6 \times 10^{-8}$ were established. We consider that the observed anisotropy is the sum of two contributions – an ‘isotropic’ term which is connected to variations in the density and gravitational potential, and a term from the anisotropic metric. A mechanism to generate the isotropic fluctuations is required, particularly on small angular scales where the Bianchi contribution is negligible, but this need not be inflationary. In our analysis we smooth the data to probe only the low- ℓ regime, and find that results are practically insensitive to the choice of spectrum for the isotropic component on large-angular scales.

Remarkably, we find a statistically significant correlation between one of these models and the *WMAP* data. Such a result may help to resolve some of the more unusual observed features of the microwave sky, albeit at the introduction of a new conundrum – the large-scale anisotropy is described at least in part by a low density Bianchi model, whereas the smaller scale fluctuations are consistent with a cosmological constant dominated, critical density model in an inflationary scenario.

2. DATA, SIMULATIONS AND TEMPLATES

In this analysis, we utilize the first-year *WMAP* data⁶ in both raw and foreground template corrected forms (Bennett et al. 2003a,b) and three heavily processed maps derived to minimize the foreground contribution in a template independent way (WILC – Bennett et al. 2003b; LILC – Eriksen et al. 2004b; TOH – Tegmark et al. 2003). For the three ILC-like maps we consider the full sky in the analysis, whereas the Kp2 or Kp0 masks (Bennett et al. 2003b) are imposed otherwise. All are smoothed to a common resolution of 5.5° FWHM and downgraded to a HEALPix⁷ resolution of $N_{\text{side}} = 32$ corresponding to harmonics up to $\ell = 64$. Such processing does not compromise the analysis since

¹ Max-Planck-Institut für Astrophysik, Karl-Schwarzschild-Str. 1, Postfach 1317, D-85741 Garching bei München, Germany; tjaffe@MPA-Garching.MPG.DE, banday@MPA-Garching.MPG.DE.

² Institute of Theoretical Astrophysics, University of Oslo, P.O. Box 1029 Blindern, N-0315 Oslo, Norway; h.k.k.eriksen@astro.uio.no, f.k.hansen@astro.uio.no.

³ JPL, M/S 169/327, 4800 Oak Grove Drive, Pasadena CA 91109; Krzysztof.M.Gorski@jpl.nasa.gov

⁴ Warsaw University Observatory, Aleje Ujazdowskie 4, 00-478 Warszawa, Poland

⁵ Wilkinson Microwave Anisotropy Probe

⁶ available at <http://lambda.gsfc.nasa.gov>

⁷ <http://www.eso.org/science/healpix/>

the Bianchi models exhibit little power outside of this ℓ -range.

To assess the statistical significance of the fits we compare our results to an ensemble of 10 000 LILC simulations, produced using the pipeline described by Eriksen et al. (2004b).

The Bianchi model templates are constructed using the formalism of Barrow et al. (1985). These models are parameterized by Ω_0 , $x = \sqrt{h/(1-\Omega_0)}$ (where h is the scale on which basis vectors change orientation), and a handedness. These models have a preferred axis along which the expansion rate is different, and about which the basis vectors themselves rotate. The smaller the x , the more rotation in a given distance traversed along a geodesic, and therefore the tighter the observed spiral pattern of induced temperature anisotropies. The smaller the Ω_0 , the larger is the asymmetry along the axis and the more focused is the structure in only one direction. In this analysis, we consider the range $0.1 \leq x \leq 10$ and $0.1 \leq \Omega_0 \leq 1$. The resulting temperature anisotropy pattern is described by Equation 4.11 of Barrow et al. (1985). The fit amplitude determines the shear $(\frac{\alpha}{H})_0$ and the vorticity $(\frac{\omega}{H})_0$ following Equation 4.8.

3. METHOD

In order to compute the correlation between the data \mathbf{d} and a template \mathbf{t} , we adopt the formalism of Górski et al. (1996) and Kogut et al. (1997). Specifically, at a given frequency we estimate a template coupling constant α by minimizing $\chi^2 = (\mathbf{d} - \alpha\mathbf{t})^T \mathbf{M}^{-1} (\mathbf{d} - \alpha\mathbf{t})$, where \mathbf{M} is the CMB signal plus noise covariance matrix. The solution to this problem (and corresponding uncertainty) is $\alpha = (\mathbf{t}^T \mathbf{M}^{-1} \mathbf{d}) / (\mathbf{t}^T \mathbf{M}^{-1} \mathbf{t})$ and $\delta\alpha = (\mathbf{t}^T \mathbf{M}^{-1} \mathbf{t})^{-1/2}$. The generalization to the multi-frequency case can be found in Górski et al. (1996). In what follows, the CMB signal covariance is specified by the *WMAP* best-fit theoretical power spectrum.

In our analysis, we must determine α over all possible models and, for each model, all relative rotations between the corresponding template and the data. Such an analysis is generally computationally demanding, but can be accelerated by a full-sky harmonic-space approach. In this case, if the noise covariance is a diagonal approximation based on the mean noise level for the map under consideration⁸ then the denominator of α is invariant under template rotation and simply computed for any given model. The numerator can then be evaluated from the convolution of the template and the “whitened” data map $\mathbf{M}^{-1}\mathbf{d}$. This operation is performed using the total convolution method of Wandelt and Górski (2001) to efficiently evaluate all such convolutions over all possible rotations.

The technique is only straightforward when considering full sky coverage. Thus, despite concerns about the effectiveness of foreground removal in the Galactic plane, we analyse the foreground-cleaned LILC map. Since chance alignments between the Bianchi template and the CMB anisotropy arising even in the absence of rotation and shear can generate non-zero correlations, we follow Kogut et al. (1997) and define the parameter $\Gamma = \alpha/\delta\alpha$

⁸ This approximation has a negligible effect on results at the *WMAP* signal-to-noise ratio.

to help reject this possibility at a given confidence and to select the best model. A reference ensemble of 10 000 LILC simulations were analysed using the above formalism to establish the distribution of α values and hence to estimate the significance of our best fit model.

Once the model and orientation axes are specified, we apply a pixel-based analysis to various combinations of the *WMAP* sky maps and impose the conservative Kp0 Galactic cut to reduce foreground contamination, in order to confirm these results. In the case of incomplete sky analysis, the amount of template structure which is masked can affect the uncertainty of the fit. Nevertheless, for the best fit orientation where the structure is largely outside the excluded Galactic Plane region, we find that the fit and its uncertainty are dominated by the CMB covariance rather than the particulars of the noise properties or sky cut. Therefore, although we calibrate using simulations strictly only applicable to the LILC result, we expect that the predicted levels of chance alignment detections should be quite robust.

4. RESULTS

The results from the analysis are summarized in Table 1 for our best fit model at $x = 0.55$ and $\Omega_0 = 0.5$, right-handed. The excess power in the southern hemisphere requires a model with low Ω_0 to focus the spiral. The cold spot and surrounding structure effectively select the particular x . See Figure 1. The best-fit Euler angles⁹ for the WILC map were found to be $(\Phi_2, \Theta, \Phi_1) = (42^\circ, 28^\circ, -50^\circ)$, and in what follows this is adopted as the best-fit axis. However, both the LILC and TOH sky maps as analysed on the full-sky yielded statistically consistent best-fit axes. This rotation places the center of the spiral structure, originally at the $-z$ axis, at $(l, b) = (222^\circ, -62)$. For each map, we tabulate the shear and vorticity, and corresponding estimate of significance as computed from the fraction of LILC simulations with a smaller α value than the observed map. The estimated shear amplitudes are consistent with a value $\sim 2.4 \times 10^{-10}$, significant at the 99.8% confidence level relative to the Monte Carlo ensemble.

In order to assess the effect of residual foreground contamination (ie. due to signals not well-traced by the foreground templates) several difference maps were constructed from the *WMAP* foreground corrected maps. The results indicate that foreground residuals are unlikely to result in spurious detections.

In Figure 1 we show (from top to bottom) the WILC map, the best-fit Bianchi model, and the difference between the two. It should be apparent that the “Bianchi corrected” map exhibits greater isotropy than the WILC data.

In Figure 2 we compare the power spectra of the original and the Bianchi-corrected V+W linear combination map¹⁰, as computed by the MASTER algorithm (Hivon et al. 2002) for the Kp2 sky coverage. It should be noted that, whilst the quadrupole amplitude is significantly increased, on average the Bianchi-corrected map has slightly less power on large scales, although both corrected and uncorrected data are in good agreement

⁹ We adopt the zyz -convention of Wandelt and Górski (2001) for the three Euler angles.

¹⁰ The *WMAP* team (Hinshaw et al. 2003) use data solely from the V- and W-bands over the spectral range $\ell < 100$.

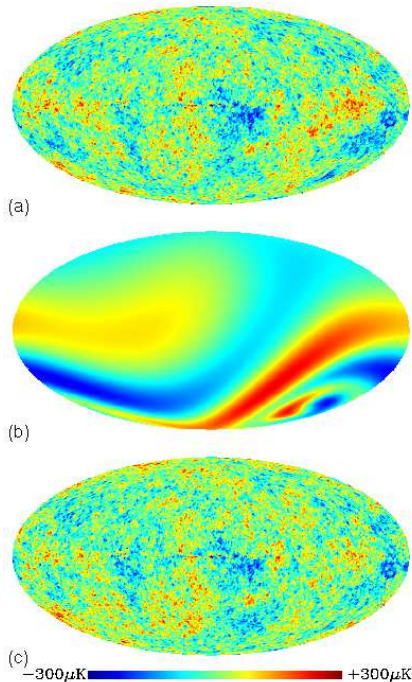


FIG. 1.— Top panel: *WMAP* Internal Linear Combination map. Middle panel: Best-fit Bianchi VII_h template (enhanced by a factor of four to show the structure). Bottom panel: Difference, *i.e.* the “Bianchi-corrected” ILC map

TABLE 1
FITTED TEMPLATE AMPLITUDES

Map	$\left(\frac{\sigma}{H}\right)_0$ ($\times 10^{-10}$)	$\left(\frac{\omega}{H}\right)_0$ ($\times 10^{-10}$)	$P(\alpha_{\text{sim}} < \alpha_{\text{obs}})^a$
WILC	2.39±0.45	6.14	99.7%
LILC	2.37±0.45	6.07	99.6%
TOH	2.25±0.45	5.76	98.6%
K ^b	2.39±0.46	6.14	99.7%
Ka ^b	2.35±0.46	6.04	99.5%
Q ^b	2.35±0.46	6.04	99.5%
V ^b	2.42±0.46	6.22	99.8%
W ^b	2.48±0.46	6.38	99.9%
Q+V+W ^{bc}	2.42±0.46	6.22	99.8%
V+W ^{bc}	2.43±0.46	6.25	99.8%
Q-V ^{bc}	-0.07 ± 0.01	0.17	-
V-W ^{bc}	-0.06 ± 0.01	0.14	-
Q-W ^{bc}	-0.12 ± 0.01	0.31	-

NOTE. — Amplitudes of the best fit Bianchi model. See text. ^a Fraction of LILC simulations with lower amplitudes. ^b Including simultaneously derived foreground corrections. ^c Using *WMAP* frequency maps pre-corrected for Galactic foregrounds.

for $\ell > 15$. More importantly, the general shape of the Bianchi-corrected spectrum is flatter than for the *WMAP* best-fit power spectrum, and in remarkable agreement with the theoretical fit made by Hansen et al. (2004a) to the northern hemisphere data (defined in the reference frame which maximises the power asymmetry) which favours a lower value for τ .

5. IMPLICATIONS

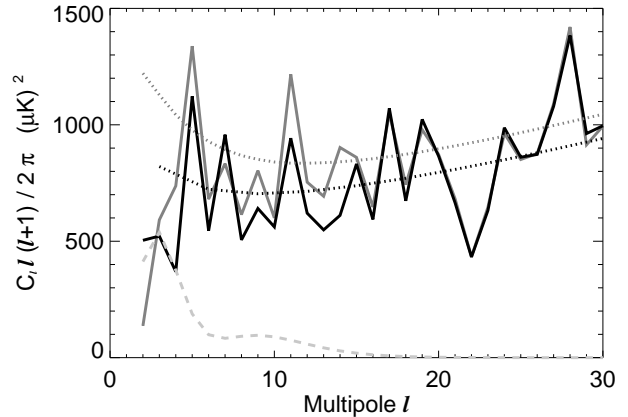


FIG. 2.— Comparison of power spectra. The gray and black solid lines show the power spectrum estimated from the co-added V+W map before and after correcting for the Bianchi template, respectively. The dotted gray and black lines shows the theoretical best-fit power-spectra from the *WMAP*-team analysis and Hansen et al. (2004a) respectively. The latter is a fit to northern hemisphere data alone. The light gray dashed line corresponds to the full sky power spectrum of the best-fit Bianchi template.

Quadrupole amplitude: The *WMAP* team suggest that the quadrupole amplitude is significantly low, although other analyses have found it to be quite acceptable (Slosar & Seljak 2004; O’Dwyer et al. 2004). As seen in Figure 2, the Bianchi-corrected V+W map has a quadrupole amplitude of $504 \mu\text{K}^2$, compared to the uncorrected amplitude of $137 \mu\text{K}^2$ and the *WMAP* theoretical best-fit spectrum value of $869 \mu\text{K}^2$. In this context, the quadrupole amplitude should no longer be considered anomalous. Whether the amplitude enhancement itself requires an unusual cancellation between the intrinsic and Bianchi-induced quadrupoles, which could also be considered a ‘fine-tuning’ of the model, is deferred to a later analysis.

Low- ℓ anomalies: An alignment between the quadrupole and the octopole has been claimed by de Oliveira-Costa et al. (2004) and Copi et al. (2004). Quantitative calculations similar to those of de Oliveira-Costa et al. (2004) and Eriksen et al. (2004b) show that a stronger planarity is expected by chance with a probability of 52% for both the $\ell = 2$ and 3 modes after subtracting the Bianchi template. The angle between the preferred directions of the $\ell = 2$ and 3 modes is 70° after subtracting the Bianchi template, compared to 12° before. Additionally, the $\ell = 5$ and 6 modes (Eriksen et al. 2004b) become less anomalous, with significances dropping to 1.5σ in both cases.

Large-scale power asymmetry: Eriksen et al. (2004a) reported that the large-scale power ($\ell \lesssim 40$) in the *WMAP* data is anisotropically distributed over two opposing hemispheres, with a significance of 3σ compared with simulations. Repeating the analysis and adopting the Kp2 sky coverage, we compare the corrected V+W *WMAP* map with 2048 simulations. We find that 13.6% of the simulations have a larger maximum power asymmetry ratio than the Bianchi-corrected map, whereas only 0.7% have a larger ratio than the uncorrected data. It is apparent that the maximum

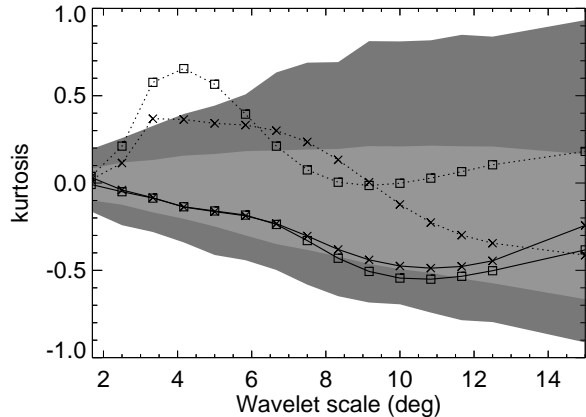


FIG. 3.— The kurtosis of the wavelet coefficients as a function of wavelet scale. The solid (dotted) lines show the results for the northern (southern) Galactic hemisphere (excluding the region where $|b| < 20^\circ$) computed from the *WMAP* ILC map. The squares (crosses) show the kurtosis before (after) correction for the Bianchi template. Grey bands indicate the two-sided 68% and 95% confidence intervals obtained from 1000 Monte-Carlo simulations.

power ratio between any two hemispheres is significantly suppressed after subtracting the Bianchi template – no asymmetry axis is found at any statistically significant level.

Wavelet kurtosis: Vielva et al. (2004) used a wavelet technique to detect an unusually cold spot ($\sim 3\sigma$ significance relative to Gaussian simulations) at Galactic coordinates $(l, b) = (207^\circ, -59^\circ)$. We repeat the analysis of Vielva et al. (2004), and compute the kurtosis of the wavelet coefficients as a function of scale from both the WILC and the corresponding Bianchi-corrected map. For computational convenience, a Galactic cut is imposed to exclude the region where $|b| < 20^\circ$. The results from this exercise are reported in Figure 3. After subtracting the Bianchi template, the southern hemisphere results are consistent with the 95% confidence intervals obtained from simulations – no non-Gaussian features are apparent.

6. CONCLUSIONS

We have considered the Bianchi type VII_h class of anisotropic cosmological models and fitted the predicted CMB temperature anisotropy patterns to the first year *WMAP* data. The results are essentially independent

of frequency or the method of foreground subtraction. A particular model with a rotation axis in the direction $(l, b) = (222^\circ, -62^\circ)$, shear $(\frac{\sigma}{H})_0 = 2.4 \times 10^{-10}$ and a right-handed vorticity $(\frac{\omega}{H})_0 = 6.1 \times 10^{-10}$ yields the best fit to the data. An ongoing analysis will improve the accuracy and completeness of the search of the model space and examine other possibly significant models.

Should this result be considered more than a curiosity? A skeptic would no doubt stress the inconsistency between those cosmological parameters describing the Bianchi anisotropy pattern (an open model with $\Omega_0 = 0.5$) and the *WMAP* best-fit cosmological power-spectrum which must account for the acoustic peaks. Yet paradoxically, it is precisely the low value for Ω_0 which is required to allow the focussing of the Bianchi anisotropy pattern into one hemisphere. The preferred Bianchi model reconciles the observed asymmetric distribution of power on large angular scales, disrupts the observed planarity and alignment of the quadrupole and octopole moments, and provides an explanation for a highly non-Gaussian signature on the sky – unexpected results given that the model was not selected based on these criteria, but solely on a statistical fit of the predicted anisotropy pattern to the *WMAP* data. Furthermore, the model is also consistent with the tentative result from Hansen et al. (2004a) that the estimated optical depth of $\tau = 0.17$ on the (nearly) full sky (Kogut et al. 2003) could in large part originate in structure associated with the southern hemisphere (in the reference frame which maximizes the power asymmetry).

While the consistency of our result on large angular scales with models for the small-scale anisotropy remains ambiguous, we note that the models considered include no dark energy contribution. A more self-consistent approach is clearly warranted, but we propose that the result is sufficiently provocative to encourage a renewed exploration of anisotropic models in a broader cosmological parameter space.

We are grateful to M. Demianski, S. Hervik, P. Mazur, and S. D. M. White for useful discussions. H. K. E. acknowledges financial support from the Research Council of Norway, including a Ph. D. scholarship. We acknowledge use of the HEALPix software (Górski et al. 2004) and of the Legacy Archive for Microwave Background Data Analysis (LAMBDA).

REFERENCES

- Bahcall, J. 2003, <http://www.sns.ias.edu/~jnb/Papers/Popular/MAPreremarks.html>
- Barrow, J. D., Juszkiewicz, R., & Sonoda, D. H. 1985, *MNRAS*, 213, 917
- Bennett, C. L. et al. 2003a, *ApJS*, 148, 1
- Bennett, C. L. et al. 2003b, *ApJS*, 148, 97
- Bunn, E. F., Ferreira, P. G., Silk, J., 1996, *PRL*, 77, 2883
- Copi, C. J., Huterer, D., & Starkman, G. D. 2004, *Phys. Rev. D*, 70, 043515
- Cruz, M., Martinez-Gonzalez, E., Vielva, P. & Cayon, L. 2005, *MNRAS*, 356, 29
- de Oliveira-Costa, A., Tegmark, M., Zaldarriaga, M., & Hamilton, A. 2004, *Phys. Rev. D*, 69, 063516
- Efstathiou, G. 2004, *MNRAS*, 348, 885
- Eriksen, H. K., Hansen, F. K., Banday, A. J., Górski, K. M., & Lilje, P. B. 2004a, *ApJ*, 605, 14
- Eriksen, H. K., Banday, A. J., Górski, K. M., & Lilje, P. B. 2004b, *ApJ*, 612, 633
- Górski, K. M., Banday, A. J., Bennett, C. L., Hinshaw, G., Kogut, A., Smoot, G. F., & Wright, E. L. 1996, *ApJ*, 464, L11
- Górski, K. M., Hivon, E., Banday A. J., Wandelt, B. D., Hansen, F. K., Reinecke, R., & Bartelmann, M., 2005, *ApJ*, 622, 759
- Hansen, F. K., Balbi, A., Banday, A. J., & Górski, K. M. 2004a, *MNRAS*, 354, 905
- Hansen, F. K., Banday, A. J., & Górski, K. M. 2004b, *MNRAS*, 354, 641
- Hinshaw, G. F. et al. 2003, *ApJS*, 148, 135
- Hivon, E., Górski, K. M., Netterfield, C. B., Crill, B. P., Prunet, S., & Hansen, F. 2002, *ApJ*, 567, 2
- Kogut, A., Hinshaw, G., Banday, A. J. 1997, *Phys. Rev. D*, 55, 4, 1901
- Kogut, A., et al. 2003, *ApJS*, 148, 161

- O'Dwyer, I. J., et al. 2004, ApJ, 617, L99
Slosar, A., & Seljak, U. 2004, Phys. Rev. D70, 083002
Hajian, A., Souradeep, T., & Cornish, N., 2005, ApJ, 618, L63
Tegmark, M., de Oliveira-Costa, A., & Hamilton, A. 2003,
Phys. Rev. D, 68, id123523
- Vielva, P., Martínez-González, E., Barreiro, R. B., Sanz, J. L., &
Cayón, L. 2004, ApJ, 609, 22
Wandelt, B. D. & Górski, K. M. 2001, Phys. Rev. D, 63, 123002